



ELSEVIER

Available online at www.sciencedirect.com

SCIENCE @ DIRECT®

Journal of Sound and Vibration 291 (2006) 491–502

JOURNAL OF
SOUND AND
VIBRATION

www.elsevier.com/locate/jsvi

Short Communication

Damping of a thin-walled honeycomb structure using energy absorbing foam

Shane C. Woody^{a,*}, Stuart T. Smith^b

^a*InsituTec Inc., Suite 103, 2750 East W.T. Harris Blvd, Charlotte, NC 28213, USA*

^b*University of North Carolina at Charlotte, Department of Mechanical Engineering, Center for Precision Metrology, 9201 University City Blvd, Charlotte, NC 28213, USA*

Received 11 March 2005; received in revised form 5 May 2005; accepted 1 June 2005

Available online 15 August 2005

Abstract

This paper presents researches into the application of energy absorbing foams as a passive damping medium to enhance the controllability for fast steering (tip-tilt) of lightweight mirrors. The direct relationship between passive damping and control highlights the merits of energy absorbing foams that have shown significant attenuation in high mode resonant frequencies (typically above 1 kHz) without adding significant mass. Studies by these researchers suggest that attenuation is coupled to standing waves through the foam. In this case study these foams have been applied to a 300 mm diameter aluminum platen that represents the final mirror geometry. In practice, mirrors for our application will be made from silicon carbide. The platen is designed with an open-back honeycomb structure and high-speed machined from 6160-T7 aluminum. Three dominant mode shapes were observed at approximately 1140, 1350 and 2100 Hz with high ' Q '. In general, the platen or any adaptive structure may require high-bandwidth dynamic control. Fundamentally, the high ' Q ' values limit the control dynamics. This paper shows the benefits of energy absorbing foams as a passive damping medium for large lightweight structures. The foams are strategically placed inside the honeycomb pockets at the back of the mirror and experimental investigations demonstrate damping coefficients up to $\xi = 0.12$ (factor of 60 improvement) compared to a $\xi \sim 0.002$ with no added passive damping in the system. Furthermore, the energy absorbing foam only adds 6% additional mass to the overall lightweight platen. As a result of this high damping coefficient, the Q values were attenuated by 25–50 dB for all high-frequency modes and as a result the controller parameters (i.e. such as

*Corresponding author.

E-mail address: shane.woody@insitutech.com (S.C. Woody).

PID) may be further optimized and provide faster settling times. Finally, the results obtained from modal testing, the relationship of damping and controller gains and potential benefits of this technique for large, lightweight structures are discussed.

© 2005 Elsevier Ltd. All rights reserved.

1. Introduction

Methods for active and passive damping are implemented regularly in electro-mechanical structures. Active damping will generate heat as in the case of electromagnetic fields or added complexity and phase lags to the overall structure as in the case of implementing piezoelectric plates to actively attenuate noise [1]. On the other hand, passive damping materials often generate less heat, can provide additional heat sinking, are simpler to implement, and are typically cost effective. Passive damping such as shear and/or squeeze film damping, viscoelastic materials [2], constrained layers, dynamic absorbers [3] and energy absorbing foams appear in many instruments and machines. Squeeze film damping typically utilizes air or, for a higher viscosity, oil constrained within a narrow gap between the movable surface and fixed frame. This can be problematic if appreciable fluid losses occur. Dynamic absorbers are very useful for large machine tools where vibration modes and frequencies are known and thus the dynamic absorber may be tuned to minimize the modal effects at desired locations around the mechanism. However, the dynamic absorber is not useful for adaptive structures where the multiple frequencies are required to be damped. Moreover, viscoelastic materials have demonstrated promising results over the years as a damping material with applications to precision machine tools [4]. However, the viscoelastic materials do not appear to attenuate well at higher frequencies (i.e. frequencies above 1 kHz) and, with relaxation, at low frequency [5]. Relaxation can also be problematic with time if it results in the material losing intimate contact with any of the surfaces.

This report addresses the potential of energy absorbing foams as a passive damping material. This relatively nascent technology has significant potential for precision motion control systems. Several types of foam compositions which have been measured for damping consist of aluminum [6], carbon [7], composites [8] and urethane [9]. The resonance and vibration attenuation is suggested to contribute to a strong coupling between the foam and structure due to standing waves in the foam. The aluminum foams have exhibited loss coefficients of up to 0.003 and densities as low as 200 kg m^{-3} . The carbon foams suggest damping coefficients of up to 0.012 and associated densities at 500 kg m^{-3} . However, the carbon foams appear to be denser and would add further weight to the overall structure. Composites continue to enhance the damping mediums with coefficient losses up to 0.04 (measurements below 100 Hz) and corresponding densities as low as 400 kg m^{-3} [10]. In recent years [11], urethane energy absorbing foams have exhibited damping coefficients up to 0.05 and densities of 104 kg m^{-3} . The tradeoff is a relatively low attenuation with frequencies below 1 kHz and the damping coefficients reduce as temperature is increased. However, this passive damping medium is still a suitable candidate for high-bandwidth motion control devices. Based upon the promising results obtained by Nayfeh et al., this paper presents results of a study of urethane foam, C-3201 (supplied by EARC Corp.) as a damping material for lightweight steering structures.

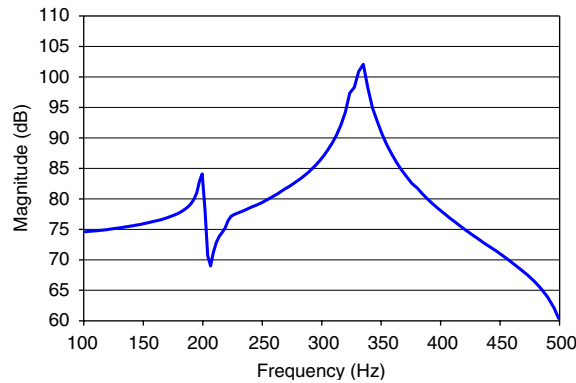


Fig. 1. Typical bode plot for a macroscale mechanical system designed with a high-frequency response.

2. Closed-loop control characteristics

In general, structural mechanisms should be damped to enhance the dynamic servo characteristics. Two methods to provide higher closed-loop control bandwidth are to

- increase the natural frequency,
- increase damping to the system.

Considering a system that is controlled by a simple integral controller. In this case, if f is the frequency at which a system has a 90° phase lag and G_I is the gain at this frequency, the integrator gain K_I that adds a further 90° lag at the first mode resonance is limited by (Fig. 1)

$$\frac{2\pi f}{K_I} \geq G_I. \quad (1)$$

Eq. (1) may be further represented in decibels as the limiting equation

$$20 \log\left(\frac{2\pi f}{K_I}\right) - 20 \log(G_I) = 0. \quad (2)$$

Therefore, 3 dB attenuation in the system gain G_I would generally correspond to a 20 percent increase in the integrator gain term. Correspondingly, an increase in the integrator gain will provide a faster closed-loop controlled response.

3. Models

Generally, the foams are considered to be effective when waves can be set up at the frequency of interest. From the work of Varanasi and Nayfeh, the complex elastic and shear moduli for the EAR C-3201 foam between frequencies of 40–2000 Hz can be obtained from the equations

$$E \approx 2075\omega^{1/2}(1 + j0.8), \quad G \approx \frac{E}{2(1 + \nu)}, \quad \nu \approx 0.36. \quad (3)$$

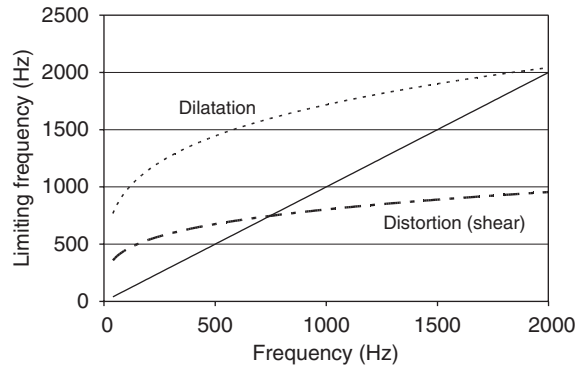


Fig. 2. Graph indicating limiting frequencies for a given wave propagation mode having a wavelength of shorter than 30 mm.

Ignoring losses, the wave speeds in dilatation, v_d , or shear, v_s , can be expressed by the equations [12]

$$v_d = \sqrt{\frac{\lambda + 2G}{\rho}}, \quad v_s = \sqrt{\frac{G}{\rho}}, \quad \lambda = \frac{\nu E}{(1 + \nu)(1 - 2\nu)}. \quad (4)$$

For a density $\rho = 104 \text{ kg m}^{-3}$, it is possible to determine a limiting low value of frequency for establishment of standing waves from the relationship

$$f > \frac{\gamma}{v}, \quad (5)$$

where f is the frequency in hertz and γ is the wavelength. For example, considering a characteristic dimension of the foam of 30 mm the limiting frequency as a function of frequency of interest is shown plotted in Fig. 2. In this a plot of both dilatation and shear modes is presented. A line at 45° indicates limiting frequency being equal to frequency of interest. Only frequencies of interest being below this line represent modes that are likely to provide substantial damping. It is apparent from this graph that for frequencies between 750 Hz and 2 kHz the dominant damping will be provided by shear waves in the foam. Above 2 kHz both modes could be established in the foam and contribute to the damping.

4. Experimentation

The structure selected for this study is an aluminum 6160-T7 circular plate with an unconventional open-back honeycomb structure of varying height, see Fig. 3. A detailed description of the application of this as a tip-tilt mirror can be found in the paper of Woody and Smith [13]. In general, three active actuators used to drive the platen contact the back plane of the platen and are equispaced by 120° and would be spaced at the Airy point positions to minimize static deformations in the platen [14]. Additionally, the varying web heights are designed to stiffen

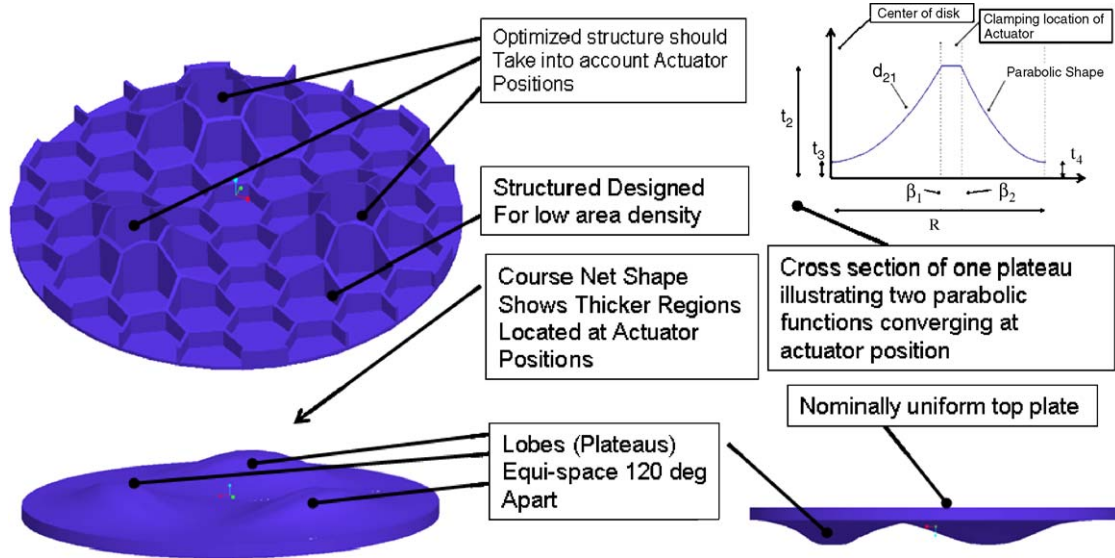


Fig. 3. Case study of an open-back honeycomb structure with variable heights.

the airy point positions. The coincident actuator locations have more material to stiffen the structure at these locations due to the applied bending moments of the actuators.

A 3D model is assessed in AnsysTM where three dominant modes were predicted at 1096, 1295 and 2085 Hz, see Fig. 4 for the first two mode shapes. As shown in Fig. 4, the largest structural bending distortion (due to the lowest mode natural frequencies) occurs along the platens' region with the shortest web heights, this being radial at 120° pitch. These bending locations correspond to radial nodes parallel with the shortest web height, Fig. 4(a), and with an additional circumferential node pattern being present in the next mode, Fig. 4(b). It is apparent that the largest distortions are radial at the lowest honeycomb thickness and around the outer diameter, thereby forming the basis for positioning of the foam damping elements.

The aluminum platen is fashioned from a flat stock referred to as a picture frame, see Fig. 5, and was high-speed machined using a Makino A55. After platen's honeycomb structure and surface contour are machined, the outer rim of the platen is machined near to the back side of the picture frame leaving a thickness of 0.15 mm. This thin floor provides the operator with the capability to easily cut the platen from the picture frame. The total machining time was approximately 2.5 h and further refining of the control codes using tool tuning and chatter theory may be optimized to less than 2 h if required.

The substrate was setup on an optical bench and impulse response measurements were assessed using an HP35665A Dynamic Signal Analyzer. A small aluminum rod with a cross-sectional area of $5.0 \times 5.0 \text{ mm}^2$ was contacted underneath the platen at the central location. This is chosen in order to contact the center node of the platen. With the platen positioned on the aluminum rod, an impulse is applied to the platen with a plastic rod and the frequencies are monitored with an acoustic microphone. The microphone's signal is transferred to the signal analyzer to measure the frequency response over 0–6.5 kHz with 800 equispaced data points. The damping foam of these

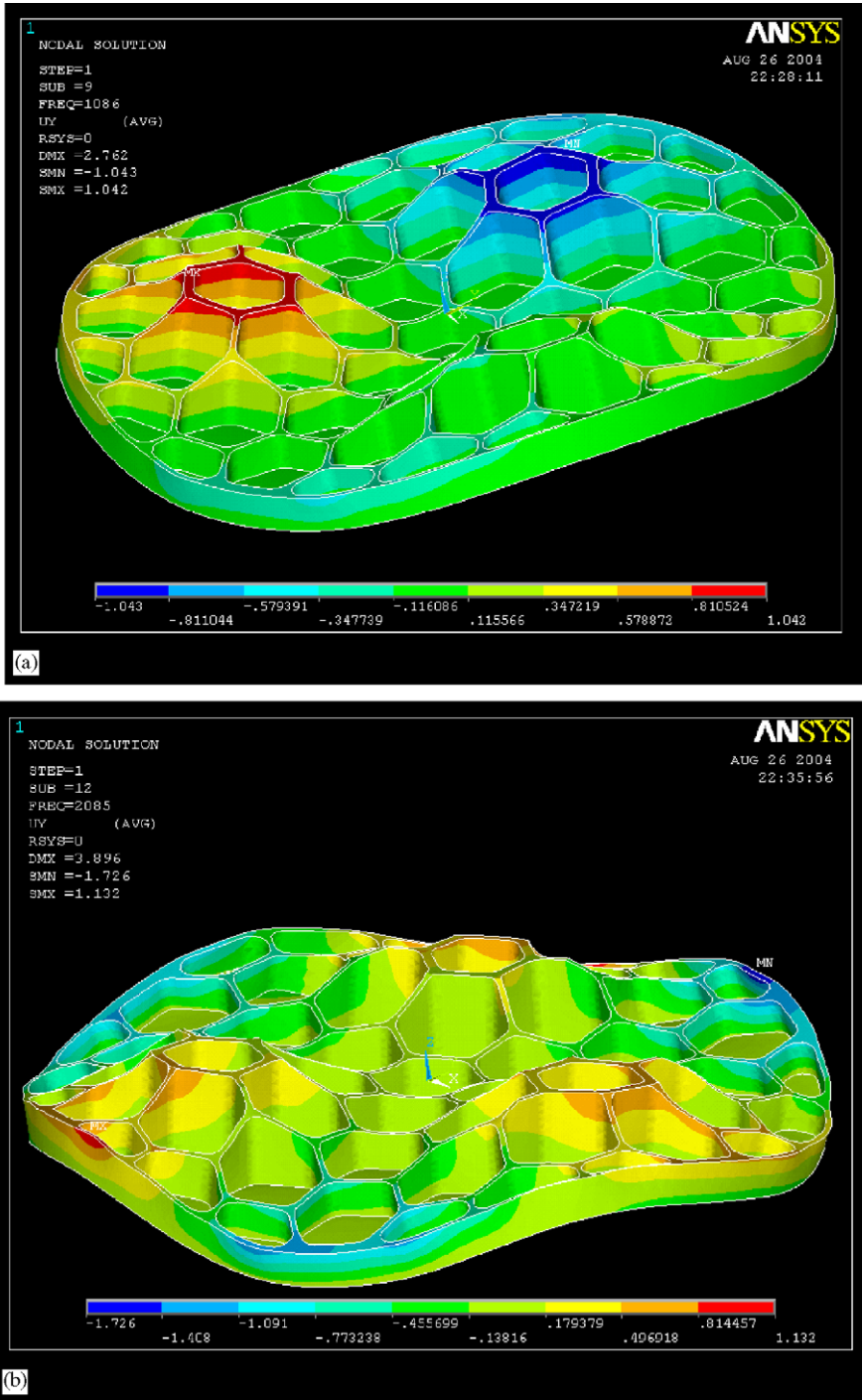


Fig. 4. FEA models showing the two dominant mode shapes at: (a) 1086 Hz, (b) 1295 Hz.

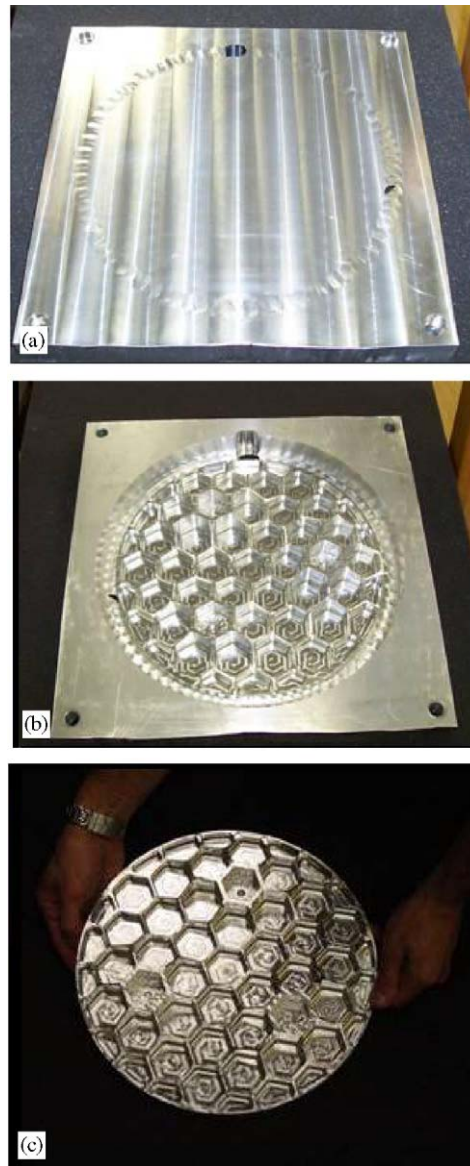


Fig. 5. Manufactured platen representing the 300 mm mirror.

experiments was cut from 12 mm thick sheet of C-3201 manufactured by EAR Specialty composites. In this series of experiments, a total of 10 damping configurations were explored and three of the configurations are illustrated in the photographs below. These three configurations depicted in Figs. 6–8 are designated as:

- *Damping configuration A*: All hexagon pockets with exception of actuator mounting and central pocket are filled with damping foam.

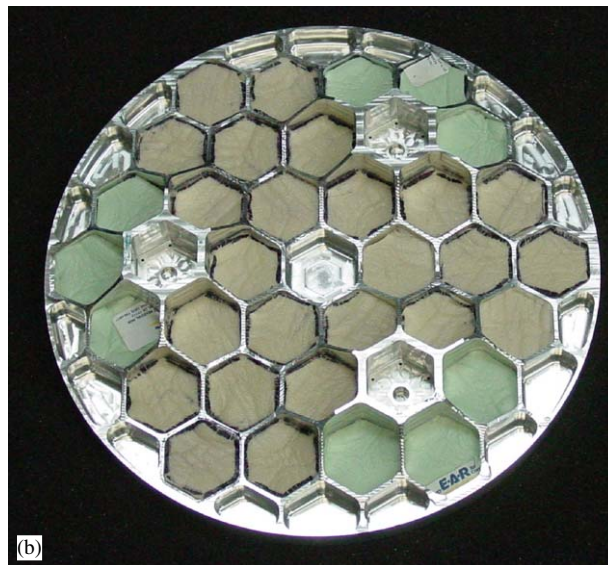
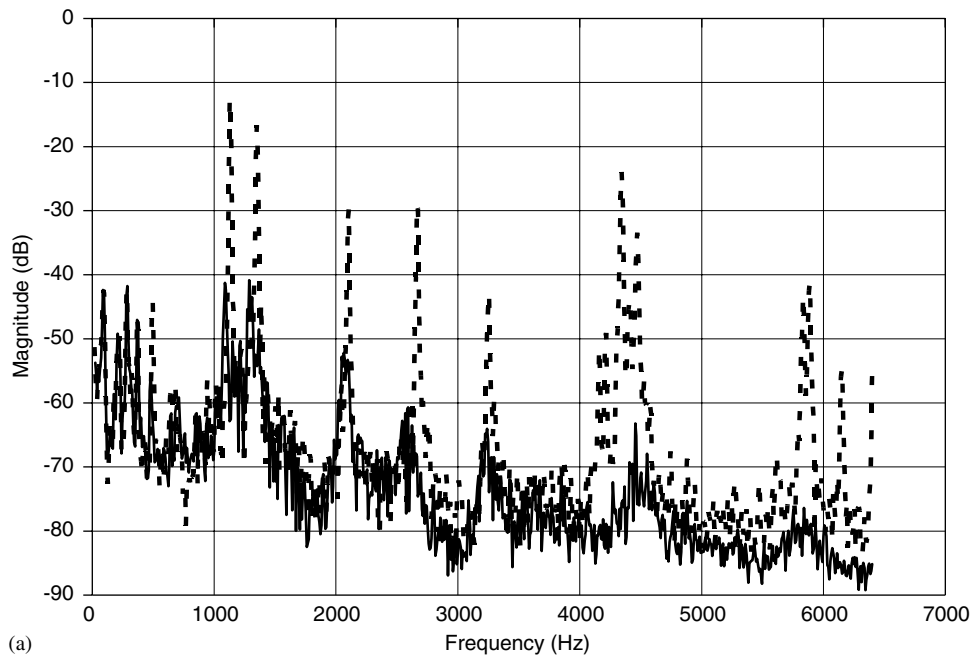


Fig. 6. Case study A with added damping in all pockets except for center and actuator locations, 73 g added mass to overall structure.

- *Damping configuration B*: The shortest web height section along the radial direction is filled.
- *Damping configuration C*: This uses configuration B and, in addition, the outer circumference of hexagon pockets are filled with damping foam.

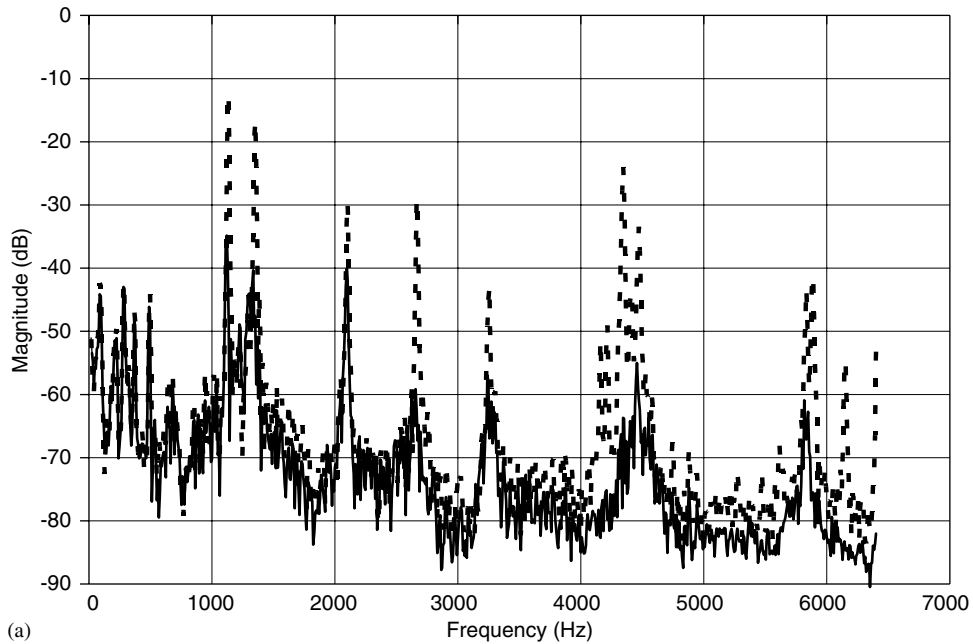


Fig. 7. Case study B with added damping along the radial direction and radial direction corresponds to smallest hexagon heights, 20 g added mass to overall structure.

The first experiment assessed the two extreme conditions with no damping and damping configuration 'A' where all available pockets are filled with foam. Based upon the FRF measurement, the harmonics were attenuated by between 25 and 50 dB with a total added mass of 73 g. In general, the added damping will benefit the control dynamics by making them less susceptible to disturbances due to a lower ' Q ' value. Two additional configurations, B and C, were assessed to determine if the amount of damping material could be reduced while sustaining a low

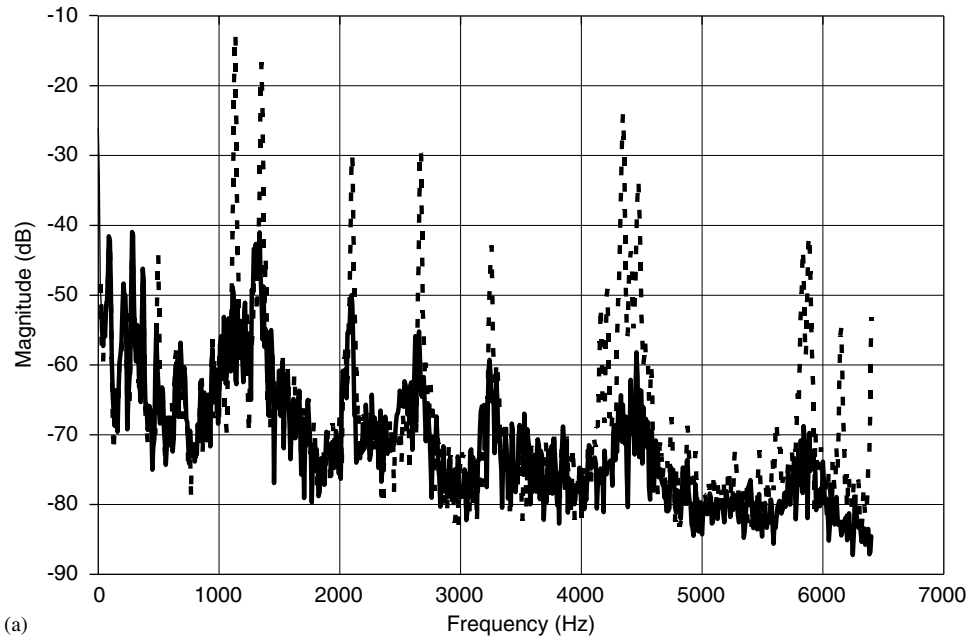


Fig. 8. Case study C with added damping along the radial direction (corresponds to smallest hexagon heights) and about the outer diameter, 53 g added mass to overall structure.

resonance ‘ Q ’ across a broad range of frequencies. These tests are shown in Figs. 7 and 8 and further described in Table 1.

Based upon the FEA and experimental analysis, the optimal locations for the energy absorbing foam lie along the path where the excitation structure is at maximum bending deformation. On average, the ‘ Q ’ values were attenuated by 30 dB for the modes between 1140 and 4340 Hz using the C-3202 foam. The logarithmic values of the impulse response were changed to a normalized magnitude and a Lorentzian function fitted locally at the peaks. The damping parameter in this

Table 1

Measured amplitude responses at the first five resonant frequencies of the honeycomb structure for different damping treatments

Damping type	Damping config.	Damping weight (g)	1140 (Hz) (dB)	1350 (Hz) (dB)	2100 (Hz) (dB)	2670 (Hz) (dB)	4340 (Hz) (dB)
None	None	0	−12.6	−16.7	−29.7	−29.0	−24.0
C-3201	A	73	−50.4	−40.8	−52.2	−66.6	−73.0
C-3201	B	20	−34.8	−42.7	−40.1	−59.9	−63.7
C-3202	C	53	−48.8	−41.0	−50.0	−55.9	−64.3

function is manually adjusted until the simulated curve has a strong correlation with the measured data. For example, the 1140 Hz peak had an initial damping ratio of $\zeta = 0.002$ prior to any added damping. Configuration C shown in Fig. 8 attenuated the Q value of the 1140 Hz peak by 34.8 dB using the damping C-3201. The same measured data again using the Lorentzian function yielded an estimate for the damping ratio of $\zeta = 0.12$. In general, the energy absorbing foam fabricated from urethane provides a factor of around 60 improvement in damping with added mass of less than 6 percent compared to the overall structure. A hybrid approach with lightweight structures and passive foams may result in an optimized solution for many high-bandwidth servo control applications.

Acknowledgments

Authors are grateful to the Missile Defense Agency (MDA) for providing funding under contract HQ0006-04-C-7063 and Dr. Arup Maji at the AFRL/Space Vehicles Directorate for his technical support throughout this project. Authors would also like to extend special thanks to Dr. Samir Nayfeh at MIT for his support and direction in this area. Furthermore, many of these investigations were carried out at UNC Charlotte's Center for Precision Metrology and authors would also like to thank Dr. Bethany Woody for her technical support in the machining of the platen.

References

- [1] M. Strassberger, H. Waller, Active noise reduction by structural control using piezo-electric actuators, *Mechatronics* 10 (2000) 851–868.
- [2] E. Kerwin, Damping of flexural waves by a constrained viscoelastic layer, *Journal of the Acoustical Society of America* 21 (1959) 952–962.
- [3] G.S. Duncan, M.F. Tummond, T.L. Schmitz, An investigation of the dynamic absorber effect in high-speed machining, *International Journal of Machine Tools and Manufacture* 45 (2005) 497–507.
- [4] E.R. Marsh, A.H. Slocum, An integrated approach to structural damping, *Precision Engineering* 18 (1996) 103–109.
- [5] R.M. Christensen, *Theory of Viscoelasticity*, Dover Publications, New York, 1982 Chapter 4.

- [6] J. Banhart, J. Baurneister, M. Weber, Damping properties of aluminum foams, *Materials Science and Engineering A* 205 (1996) 221–228.
- [7] Konstantin Maslov, Vikram K. Kinra, Damping capacity of carbon foam, *Materials Science and Engineering A* 367 (2004) 89–95.
- [8] M.C. Gui, D.B. Wang, J.J. Wu, G.J. Yuan, C.G. Li, Deformation and damping behaviors of foamed Al–Si–SiCp composite, *Materials Science and Engineering A* 286 (2000) 282–288.
- [9] Kripa K. Varanas and Samir A. Nayfeh, Damping of flexural vibration by low-density foams and granular materials, *Proceedings of DETC'03, ASME Design Engineering Technical Conference*, Vol. 5, 2003, pp. 1897–1905.
- [10] W. Jiejun, L. Chenggong, W. Dianbin, G. Manchang, Damping and sound absorption properties of particle reinforced Al matrix composite foams, *Composites Science and Technology* 63 (2003) 569–574.
- [11] K.K. Varanasi, S.A. Nayfeh, Damping of flexural vibration in the plane of lamination of elastic–viscoelastic sandwich beams, *Journal of Sound and Vibration* 276 (2004) 689–711.
- [12] A.E.H. Love, *A Treatise on the Mathematical Theory of Elasticity*, Dover Publications, New York, 1944 Chapter 13.
- [13] S.C. Woody, S.T. Smith, Steering mirror design and dynamic controls for a dual actuation platform using high-strain actuators, *Proceedings of the 46th AIAA Structures, Structural Dynamics and Materials Conference*, 2005.
- [14] G.D. Dew, The measurement of optical flatness, *Journal of Scientific Instruments* 43 (1966) 409–415.